LAWRENCE
LIVERMORE
NATIONAL
LABORATORY

LLNL-TR-665562

A Model-Based Approach to Scintillator/Photomultiplier System Characterization

J. V. Candy

December 17, 2014

Disclaimer

This work performed under the auspices of the U.S. Department of Energy by Lawrence Livermore National Laboratory under Contract DE-AC52-07NA27344.

A MODEL-BASED APPROACH

TO

SCINTILLATOR/PHOTOMULTIPLIER SYSTEM CHARACTERIZATION

James V Candy

Scintillator/photomultiplier systems are prevalent in many instruments to measure a variety on nuclear events. When gamma energy from a nuclear event irradiates the scintillator, event radiation interacts with the scintillator material generating photons which are detected by the photomultiplier tube (PMT) [1], [2]. The PMT photoelectrons or photocathode current is amplified in the PMT by a number of dynode stages producing a total charge out for a given radiation flux into scintillator. The resulting current is converted to a voltage when passed through a typical load impedance. This voltage is attenuated and provided as input to a digitizer through a variety of signal conditioners (filters, amplifiers, receivers) before analog-to-digital conversion. In this report, we concentrate on the development of analytic models for the scintillator/photomultiplier system and develop both a (1) statistical simulator; and (2) a model-based signal processor to extract the desired signal information while rejecting the noise and uncertainty. We develop the model analytically, transform it to the model-based framework (state-space [3], [4]), and then use actual experimental data to fit the model and apply it to our processing problem.

A simple diagram of a scintillation/photomultiplier system is shown in Fig. 1. As an incident alpha particle interacts with the scintillator crystal, typically sodium iodide (NaI), the kinetic energy of the particle is converted into detectable light through the "prompt fluorescence" property of the particular crystal. The light (photons) then strike the thin photocathode material of the photomultiplier causing it to emit a photoelectrons which are focused (electrostatically) onto a series of electron multiplier stages or dynodes which amplify the converted energy that is eventually collected at the multiplier anode. These dynodes are electrodes that emit a number of secondary electrons in response to the absorption of a single photoelectron thereby amplifying the original photoelectron from stage-to-stage with a typical gain factor of 10^7 [1]. These electrons are then collected at the anode of the photomultiplier tube (PMT) producing the output voltage pulse. It is this pulse that is of most interest, since it is proportional to the original incident photon energy emitted from the unknown source.

The shape of the voltage pulse at the PMT output is governed by the prompt fluorescence intensity of the scintillator crystal at a time *t* following the initial excitation with an exponential decay time τ_s such that the intensity is given (simply) by

$$i(t) = i_o e^{-t/\tau_s} \tag{1}$$

where τ_s is usually a few nanoseconds. A full description of the output pulse must also take the rise time at the anode into account which is usually around 3 to 4 times larger (faster) than the fall, say τ_a. Then the overall voltage output pulse of the scintillator system is given by [2]

$$i(t) = i_o \left(e^{-t/\tau_a} - e^{-t/\tau_s} \right) \tag{2}$$

Using the parameters for a plastic scintillator from [2] ($\tau_s = 1.7\text{ns}$, $\tau_a = 0.2\text{ns}$, $i_o = 1000$), the resulting pulse is shown in Fig. 2. Next we develop the model of Eq. 2 from an equivalent electrical circuit representation.

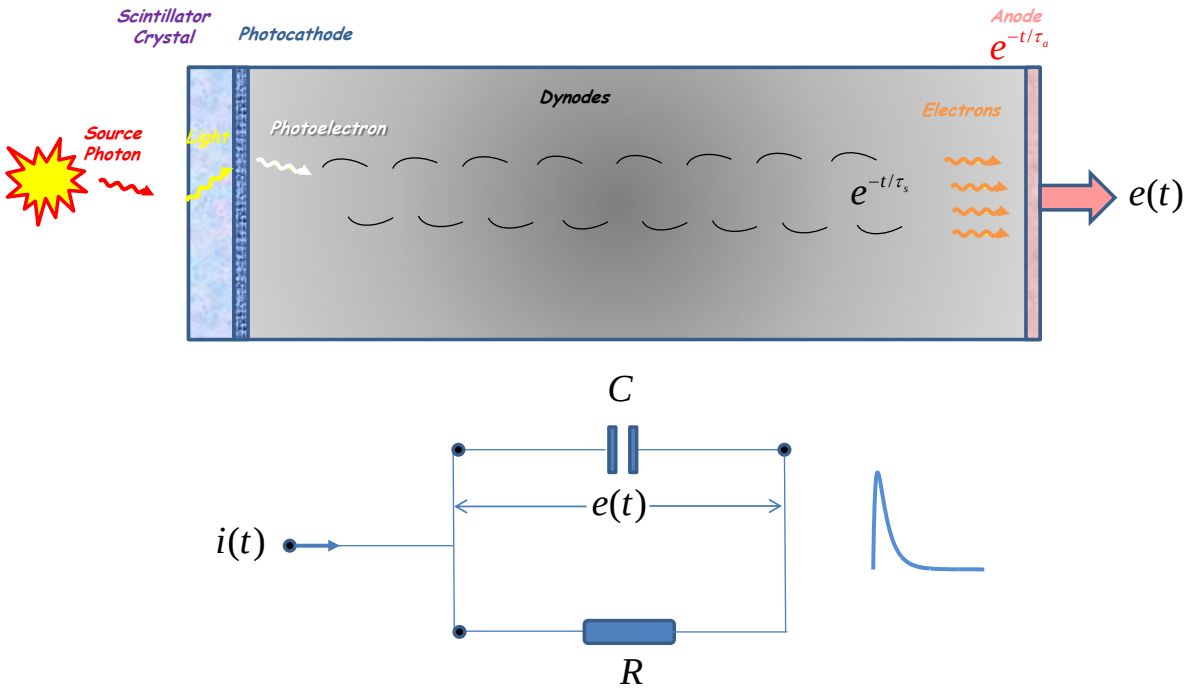

Scintillator/Photomultiplier System with Equivalent Circuit Model

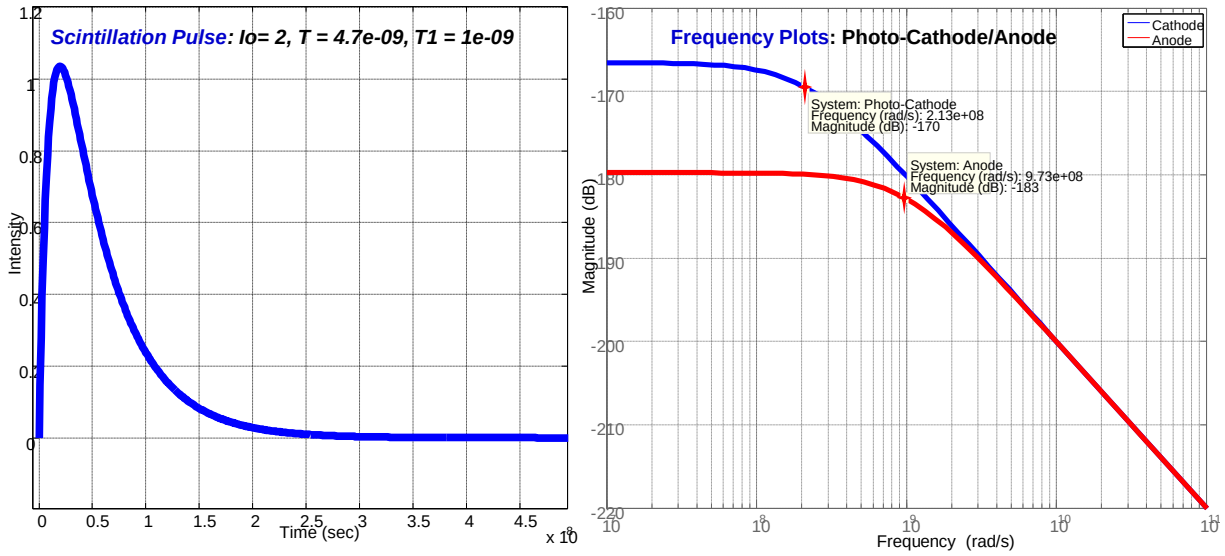

Typical Scintillator/Photomultiplier Response: (a) Pulse. (b) Bode plot.

SCINTILLATION PULSE SHAPE MODEL

Following Knoll [2], the shape of the voltage pulse at the anode of the PMT following an event depends on the time constant of the anode circuit τ_a and the decay time of the scintillator τ_s . For our application we would like a very fast output pulse and therefore the design calls for the anode circuit time constant τ_a to be much smaller than that of the scintillator decay time. The equivalent anode circuit (ideal) can be realized as a simple parallel resistor/capacitor connection with the input current modeling the fluorescence as a simple exponential as in Eq. 1. Here the lumped capacitance (C) represents that of the anode and cable connections as well as the circuit input capacitance while the resistance (R) is a physical resistor or the input impedance of the circuit load. The input electron current arriving at the PMT anode is given by Eq. 1 with the initial current a function of the total charge Q collected and given by

$$i_o = \frac{Q}{\tau_s} \tag{3}$$

Thus, writing the node equation using Kirchhoff's current law [3] we have that total input current is the sum of the currents through the resistance and capacitance

$$i(t) = i_R(t) + i_C(t) \tag{4}$$

or

$$i(t) = C\frac{de(t)}{dt} + \frac{e(t)}{R} \tag{5}$$

The solution of this simple differential equation follows using Laplace transforms [3], that is,

$$I(s) = CsE(s) - Ce(0) + \frac{E(s)}{R} \tag{6}$$

or

$$E(s) = \frac{I(s)/C}{\left(s + 1/RC\right)} - \frac{e(0)}{\left(s + 1/RC\right)} = \frac{I(s)/C}{\left(s + \frac{1}{\tau_a}\right)} - \frac{e(0)}{\left(s + \frac{1}{\tau_a}\right)} \quad \text{for } \tau_a = \text{anode } RC \text{ time constant} \tag{7}$$

The transform of the scintillator decay is

$$I(s) = \frac{i_o}{\left(s + \frac{1}{\tau_s}\right)} \tag{8}$$

Assuming zero initial voltage across anode ($e(0) = 0$), then substituting for $I(s)$ in Eq. (7), we obtain

$$E(s) = \frac{i_o/C}{\left(s + \frac{1}{\tau_a}\right)\left(s + \frac{1}{\tau_s}\right)} \tag{9}$$

The cascaded system is shown in Fig. 3 along with the individual transfer functions and corresponding impulse responses.

The *inverse* Laplace transform ($L^{-1}\{\bullet\}$) of Eq. (9) can be obtained using the partial fraction (residue theorem) approach to give the final solution as [3]

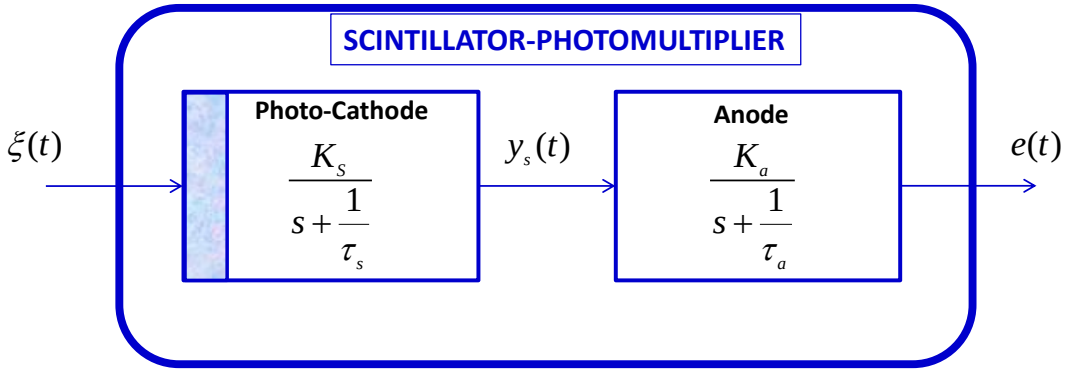

Photo-Cathode: Anode:

$$H_s(s) := \frac{Y_s(s)}{\xi(s)} = \left(\frac{K_S}{s+\frac{1}{\tau_s}} \right) \qquad H_a(s) := \frac{E(s)}{Y_s(s)} = \left(\frac{K_a}{s+\frac{1}{\tau_a}} \right)$$

$$h_s(t) = K_s e^{-\frac{t}{\tau_s}} \qquad h_a(t) = K_a e^{-\frac{t}{\tau_a}}$$

Figure 3. *Cascaded Scintillator/Photomultiplier System Model: (a) Diagram. (b) Transfer function/Impulse response.*

$$e(t) = \left(\frac{i_o}{C}\right) \; L^{-1}\left\{ \frac{K_a}{\left(s+\frac{1}{\tau_a}\right)} + \frac{K_S}{\left(s+\frac{1}{\tau_s}\right)} \right\} = \left(\frac{i_o}{C}\right)\left[K_a e^{-t/\tau_a} + K_s e^{-t/\tau_s} \right] \qquad (10)$$

where

$$K_a = \frac{\lim}{s \to -\frac{1}{\tau_a}} \left(s+\frac{1}{\tau_a} \right) E(s) = \frac{1}{-\frac{1}{\tau_a}+\frac{1}{\tau_s}} = \frac{\tau_a \tau_s}{\tau_a - \tau_s}; K_S = \frac{\lim}{s \to -\frac{1}{\tau_s}} \left(s+\frac{1}{\tau_s} \right) E(s) = \frac{1}{\frac{1}{\tau_a}-\frac{1}{\tau_s}} = -\frac{\tau_a \tau_s}{\tau_a - \tau_s}$$

or simply

$$e(t) = \left(\frac{i_o}{C}\right)\left(\frac{\tau_a \tau_s}{\tau_a - \tau_s}\right)\left[e^{-t/\tau_a} - e^{-t/\tau_s}\right] = \frac{Q}{C}\left(\frac{\tau_a}{\tau_a - \tau_s}\right)\left[e^{-t/\tau_a} - e^{-t/\tau_s}\right] \tag{11}$$

Finally we have that the output voltage signature for the scintillator is

$$e(t) = K_{as}\left[e^{-t/\tau_a} - e^{-t/\tau_s}\right] \quad \text{for} \quad K_{as} := \frac{Q}{C}\left(\frac{\tau_a}{\tau_a - \tau_s}\right) \tag{12}$$

Thus, the output voltage pulse $e(t)$ has the identical form of the physical model of Eq. (2).

MODEL-BASED FORM: STATE-SPACE MODEL

In order to develop our model-based simulation for the scintillator, we choose to use the state-space[1] representation which simply put means that we develop the underlying differential equation governing our scintillator model of Eq. (5) which is easily obtained from the cascade of sub-systems shown in Fig. 3.

The photo-cathode system is governed by the differential equation that evolves from the transfer function:

$$\begin{aligned} &\frac{d}{dt}i(t) + \frac{1}{\tau_s}i(t) = K_s\xi(t) && \text{[Photoelectron Current]} \\ &y_s(t) = i(t) && \text{[Output Current]} \end{aligned} \tag{13}$$

where ξ is the input excitation (assumed to be an impulse-like signal).

The anode of the photomultiplier is modeled by the RC-circuit analyzed in the previous section and is governed by the Kirchhoff current relation of Eq. (5)

$$\begin{aligned} &\frac{d}{dt}e(t) + \frac{1}{\tau_a}e(t) = K_a i(t) \quad \text{for} \quad \tau_a = RC && \text{[Anode Voltage]} \\ &y_a(t) = e(t) && \text{[Output Voltage]} \end{aligned} \tag{14}$$

[1] States are simply rewriting the n-th order differential equation into n first-order differential equations.

If we define the state vector $\mathbf{x}(t) := \left[i(t) \quad | \quad e(t) \right]^T$, then we obtain the vector-matrix equation

$$\frac{d}{dt}\begin{bmatrix} i(t) \\ -- \\ e(t) \end{bmatrix} = \underbrace{\begin{bmatrix} -\frac{1}{\tau_s} & 0 \\ 0 & -\frac{1}{\tau_a} \end{bmatrix}}_{\text{states}} \begin{bmatrix} i(t) \\ -- \\ e(t) \end{bmatrix} + \underbrace{\begin{bmatrix} K_s \\ -- \\ \frac{K_a}{C} \end{bmatrix}}_{\text{input}} u(t) \qquad \text{[States]}$$

$$\underset{\text{output}}{y(t)} = \begin{bmatrix} 0 & | & 1 \end{bmatrix} \begin{bmatrix} i(t) \\ -- \\ e(t) \end{bmatrix} \qquad \text{[Measurement]} \tag{15}$$

or simply

$$\begin{aligned} \dot{\mathbf{x}}(t) &= \mathbf{A}\mathbf{x}(t) + \mathbf{B}u(t) \\ y(t) &= \mathbf{C}\mathbf{x}(t) \end{aligned} \tag{16}$$

the usual state-space representation of a linear time-invariant system with A, B, C the respective $N_x \times N_x$, $N_x \times \mathrm{N}_u$, $N_y \times N_x$ system, input and output matrices [4] and having the corresponding impulse response $H(t)$ and transfer function $H(s)$ given by $H\left(t\right) = C\, e^{A(t-\tau)}B$ and $H(s) := L^{-1}\left\{H(t)\right\} = C(sI - A)^{-1}B$, respectively. The transfer function (zero initial conditions) follows directly by taking the inverse Laplace transform of Eq. (16) and combining, that is,

$$\begin{aligned} sX(s) - AX(s) &= BU(S) \\ Y(s) &= CX(s) \end{aligned} \tag{17}$$

Combining terms and solving using $(sI - A)^{-1}$ gives the transfer function directly. For our problem of Eq. (15), we obtain

$$H(s) = C(sI - A)^{-1}B = \underbrace{\begin{bmatrix} 0 & | & 1 \end{bmatrix}}_{C} \underbrace{\begin{bmatrix} s + \frac{1}{\tau_s} & 0 \\ 0 & s + \frac{1}{\tau_a} \end{bmatrix}^{-1}}_{sI - A} \underbrace{\begin{bmatrix} K_s \\ \cdots \\ K_a \end{bmatrix}}_{B} \tag{18}$$

which completes the state-space representation of the scintillator-photomultiplier system.

MODEL-BASED FORM: SAMPLED-DATA STATE-SPACE MODEL

The continuous-time state-space model requires numerical integration. Since the signals are to be digitized, a more reasonable model can be achieved using sampled-data theory to transform directly from continuous to discrete-time systems [3], [4].

The solution to the deterministic state-space model of Eq. (16) is given by

$$\mathbf{x}(t) = \mathbf{\Phi}(t, t_o)\mathbf{x}(t_o) + \int_0^t \mathbf{\Phi}(t, \tau)\mathbf{B_c}\mathbf{u}(\tau)d\tau \tag{19}$$

where the state transition matrix, $\mathbf{\Phi}$, and the subscript "c" (continuous-time) given by

$$\mathbf{\Phi}\left(t, t_o\right) = e^{\mathbf{A_c}(t-t_o)} \tag{20}$$

Sampled-data (A/D) implies that $t \to t_k$ and therefore $\mathbf{\Phi}\left(t_k, t_o\right) = e^{\mathbf{A_c}(t_k-t_o)}$ and the solution of Eq. (19) becomes

$$\mathbf{x}(t_k) = \mathbf{\Phi}\left(t_k, t_{k-1}\right)\mathbf{x}(t_{k-1}) + \int_{t_{k-1}}^{t_k} \mathbf{\Phi}\left(t_k, \tau\right)\mathbf{B_c}\mathbf{u}(\tau)d\tau \tag{21}$$

Define the sample data system with the input assumed piecewise-constant (p.w.c.), that is,

$u(t_{k-1}) \le u(t) < u(t_k)$ and $\mathbf{B} := \int_{t_{k-1}}^{t_k} \mathbf{\Phi}\left(t_k, \tau\right)\mathbf{B_c}d\tau$ leading to the discrete *sampled-data system* given by

$$\mathbf{x}(t_k) = \mathbf{A}\mathbf{x}(t_{k-1}) + \mathbf{B}\mathbf{u}(t_{k-1}) \tag{22}$$

where

$$\begin{aligned} \mathbf{A} &:= e^{\mathbf{A_c}(t_k - t_{k-1})} = e^{\mathbf{A_c}\Delta t_k} \text{ where } \Delta_k := t_k - t_{k-1} \\ \mathbf{B} &:= \left(\int_{t_{k-1}}^{t_k} e^{\mathbf{A_c}(t_k - \tau)} d\tau \right) \times \mathbf{B_c} \end{aligned} \tag{23}$$

and the corresponding measurement system is simply digitized to give

$$\mathbf{y}(t_k) = \mathbf{C}\mathbf{x}(t_k) \tag{24}$$

We developed a simulation of this system and the results are shown in Fig. 4 where we see the states the current *i* and the voltage *v* and the output *y*. Here the input was an impulse function.

MODEL-BASED FORM: GAUSS-MARKOV STATE-SPACE MODEL

The deterministic model of the scintillator/photomultiplier system lacks because of the presence of uncertainties not captured in its characterization. The state-space model of Eq. (16) can easily be extended to capture both modeling and measurement uncertainties using a Gauss-Markov representation (see [4] for more details) given by

$$\begin{aligned} \dot{\mathbf{x}}(t) &= \mathbf{A}\mathbf{x}(t) + \mathbf{B}u(t) + \mathbf{w}(t) \\ y(t) &= \mathbf{C}\mathbf{x}(t) + \mathbf{v}(t) \end{aligned} \tag{25}$$

where A, B, C are the matrices defined above and $\mathbf{w}, \mathbf{v}$ are zero Gaussian noise/uncertainty vectors of appropriate dimension with covariance matrices, $\mathbf{R}_{ww}, \mathbf{R}_{vv}$ respectively and $\mathbf{x}(0) \sim N(\bar{\mathbf{x}}(0), \mathbf{P}(0))$ [2] . It can further be shown that the corresponding state and measurement statistics satisfy the following relations, that is, defining $m_x(t) := E\{x(t)\}$, $m_y(t) := E\{y(t)\}$ and $P_{xx}(t) := \mathrm{cov}(x(t)), R_{yy}(t) := \mathrm{cov}(y(t))$ we have the following set of equations (see [4] for more details):

$$\begin{aligned} \dot{\mathbf{m}}_x(t) &= \mathbf{A}\mathbf{m}_x(t) + \mathbf{B}\mathbf{u}(t) && \text{[State Mean]} \\ \dot{\mathbf{P}}_{xx}(t) &= \mathbf{A}\mathbf{P}_{xx}(t) + \mathbf{P}_{xx}(t)\mathbf{A}^T + \mathbf{R}_{ww} && \text{[State Covariance]} \\ \dot{\mathbf{m}}_y(t) &= \mathbf{C}\mathbf{m}_x(t) && \text{[Measruement Mean]} \\ \mathbf{R}_{yy}(t) &= \mathbf{C}\mathbf{P}_{xx}(t)\mathbf{C}^T + \mathbf{R}_{vv} && \text{[Measurement Covariance]} \end{aligned} \tag{26}$$

From these relations, the Gauss-Markov representation enables us to capture the uncertainties of the underlying process.

Since we are using *digitized* data, then a sampled-data representation of this continuous-time system will be a better approach to characterizing this system. Therefore, using the same approach of the deterministic system given in Eq. (22) we obtain

[2] Here the notation *z~N(m,V)* means *z* is Gaussian distributed with mean *m* and covariance *V*.

$$\mathbf{x}(t_k) = \mathbf{A}\mathbf{x}(t_{k-1}) + \mathbf{B}\mathbf{u}(t_{k-1}) + \mathbf{B}_\mathbf{w}\mathbf{w}(t_{k-1})$$
$$\mathbf{y}(t_k) = \mathbf{C}\mathbf{x}(t_k) + \mathbf{v}(t_k) \tag{27}$$

where both additive process and measurement noises are zero-mean, Gaussian processes with respective covariance matrices are $R_{ww}(t_{k-1})$, $R_{vv}(t_k)$ with

$$\mathbf{A} := e^{\mathbf{A}_\mathbf{c}(t_k - t_{k-1})}$$
$$\mathbf{B} := \left(\int_{t_{k-1}}^{t_k} e^{\mathbf{A}_\mathbf{c}(t_k - \tau)} d\tau \right) \times \mathbf{B}_\mathbf{c} \tag{28}$$
$$\mathbf{B}_w := \left(\int_{t_{k-1}}^{t_k} e^{\mathbf{A}_\mathbf{c}(t_k - \tau)} d\tau \right)$$

The corresponding statistics are given by (see [4] for more details):

$$\mathbf{m}_x(t_k) = \mathbf{A}\mathbf{m}_x(t_{k-1}) + \mathbf{B}\mathbf{u}(t_{k-1}) \quad \text{[State Mean]}$$
$$\mathbf{P}_{xx}(t_k) = \mathbf{A}\mathbf{P}_{xx}(t_{k-1})\mathbf{A}^T + \mathbf{R}_{ww}(t_{k-1}) \quad \text{[State Covariance]} \tag{29}$$
$$\mathbf{m}_y(t_k) = \mathbf{C}\mathbf{m}_x(t_k) \quad \text{[Measruement Mean]}$$
$$\mathbf{R}_{yy}(t_k) = \mathbf{C}\mathbf{P}_{xx}(t_k)\mathbf{C}^T + \mathbf{R}_{vv}(t_k) \quad \text{[Measurement Covariance]}$$

for process noise covariance given by

$$\mathbf{R}_{\mathbf{ww}}(t_k) = \int_{t_{k-1}}^{t_k} \left(e^{A_\mathbf{c}(t_k - \tau)} \right) \times \mathbf{R}_{ww}(\tau) \times \left(e^{A_\mathbf{c}(t_k - \tau)} \right)^T d\tau \tag{30}$$

Next we illustrate this approach by simulating the scintillator/photomultiplier system *with* uncertainties.

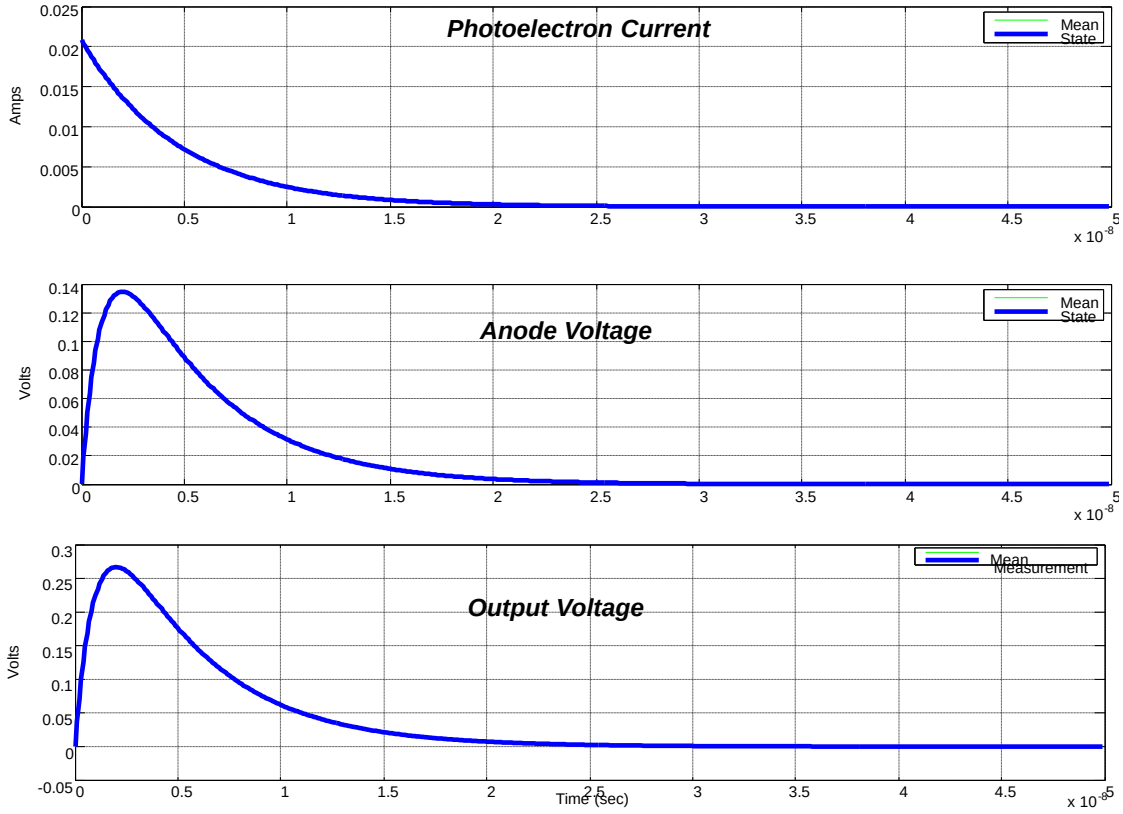

Figure 4. *Deterministic state-space model output for cascaded scintillator/photomultiplier system simulation.*

GAUSS_MARKOV SIMULATION: SCINTILLATION PULSE SHAPE MODEL

We performed a Gauss-Markov simulation of the scintillation/photomultiplier system of the previous subsection using the set of parameters estimated (see next subsection) from our average PMT data set: $K_{ab} = 1.98, \tau_a = 1.03 \times 10^{-9}$ sec, $\tau_s = 4.7 \times 10^{-9}$ sec. We still used the impulse excitation and added zero mean Gaussian noise with respective covariances. The results are shown in Fig. 5.

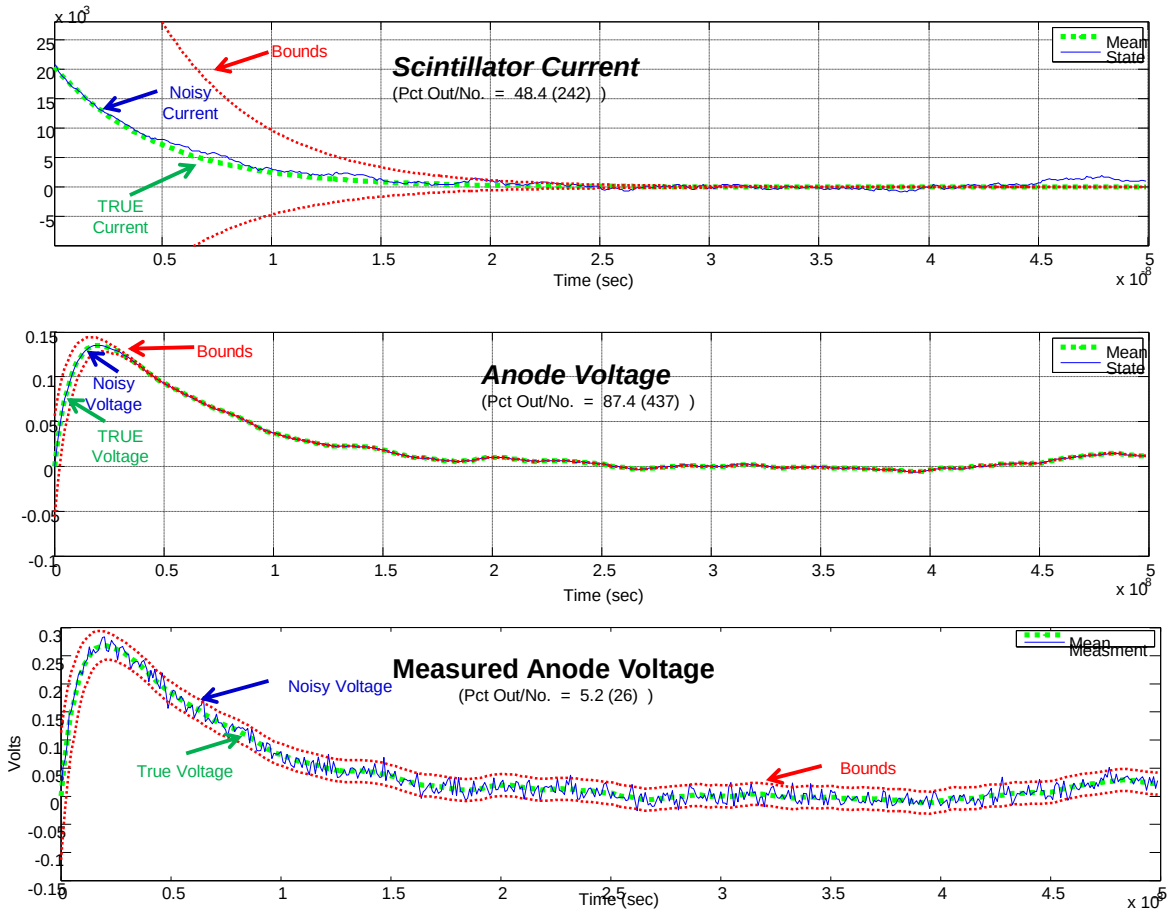

Figure 5. *Stochastic state-space model output for cascaded scintillator/photomultiplier system simulation.*

PARAMETER ESTIMATION: SCINTILLATION PULSE SHAPE MODEL

In order to develop a simulation of the scintillator output, we must first estimated the parameters (K_{ab}, τ_a, τ_b) from the measured response (averaged) of our scintillator and photomultiplier system shown in Fig. 3. We apply a nonlinear optimization technique available in MATLAB using the well-known Nelder-Meade algorithm [5]. The results of the fit are shown in Fig. 6 illustrating a reasonable estimate of the response. The final parameter estimates are: $K_{ab} = 1.98, \tau_a = 1.03\times10^{-9}$ sec, $\tau_s = 4.7\times10^{-9}$ sec and are used in the simulation model for each of our photomultiplier channels.

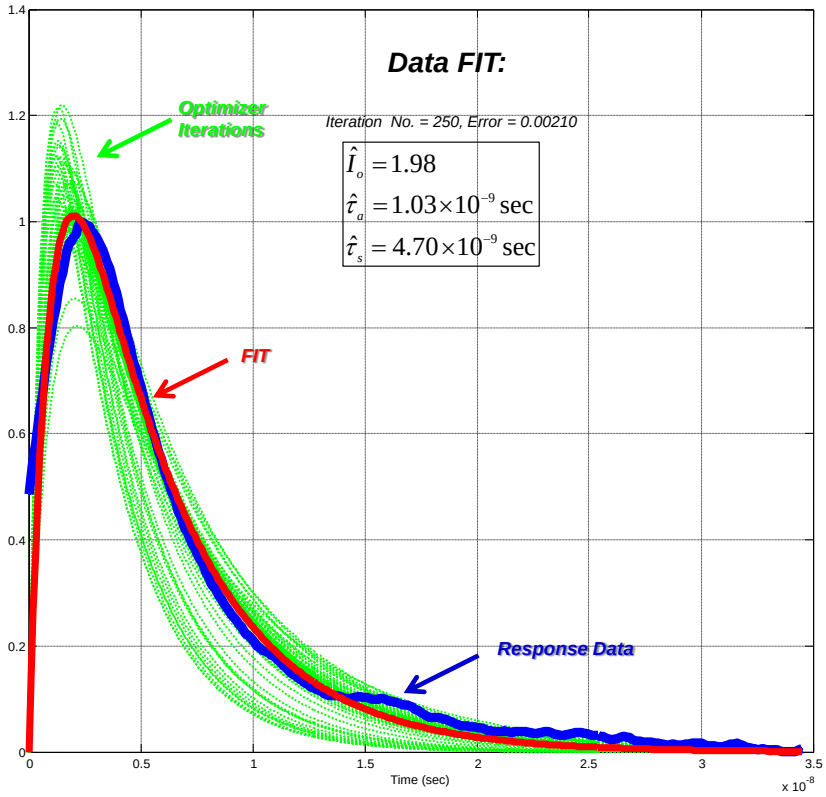

Figure 6. *Parameter estimation for scintillator voltage response: iterates (green), fit (red) and raw response (blue).*

MODEL-BASED PROCESSOR: SCINTILLATION /PHOTOMULTIPLIER SYSTEM

Now that we have developed a stochastic representation of the scintillator/photomultiplier system, which is commonplace in practice with the underlying uncertainties (noise, parameters, etc.), we now develop a processor capable of using these models and extracting the desired signals from the noisy, uncertain measurement data. Under the Gauss-Markov assumptions, there exists and *optimal* model-based solution---the Kalman filter [4]. The derivation of the Kalman filter is beyond the scope of this study, so we just present the *sequential* sampled-data algorithm in Table 2.0 and apply it to the noisy scintillator/photomultiplier data of the previous section.

Table 2.0: MODEL-BASED PROCESSOR (Kalman Filter)

$$\hat{\mathbf{x}}(t_k \mid t_{k-1}) = \mathbf{A}\hat{\mathbf{x}}(t_{k-1} \mid t_{k-1}) + \mathbf{B}\mathbf{u}(t_k) \quad \text{[State Prediction]}$$

$$\tilde{\mathbf{P}}(t_k \mid t_{k-1}) = \mathbf{A}\tilde{\mathbf{P}}(t_k \mid t_{k-1})\mathbf{A}^{\mathbf{T}} + \mathbf{R}_{\mathbf{ww}}(t_{k-1}) \quad \text{[State Error Covariance Prediction]}$$

$$\hat{\mathbf{y}}(t_k \mid t_{k-1}) = \mathbf{C}\hat{\mathbf{x}}(t_k \mid t_{k-1}) \quad \text{[Measurement Prediction]}$$

$$\boldsymbol{\varepsilon}(t_k \mid t_{k-1}) = \mathbf{y}(t_k - \hat{\mathbf{y}}(t_k \mid t_{k-1}) \quad \text{[Innovations Prediction]}$$

$$\mathbf{R}_{\boldsymbol{\varepsilon\varepsilon}}(t_k \mid t_{k-1}) = \mathbf{C}\tilde{\mathbf{P}}(t_k \mid t_{k-1})\mathbf{C}^{\mathbf{T}} + \mathbf{R}_{\mathbf{vv}}(t_k) \quad \text{[Innovations Covariance Prediction]}$$

$$\mathbf{K}(t_k) = \tilde{\mathbf{P}}(t_k \mid t_{k-1})\mathbf{C}^{\mathbf{T}}\mathbf{R}_{\boldsymbol{\varepsilon\varepsilon}}^{\mathbf{-1}}(t_k \mid t_{k-1}) \quad \text{[Gain Prediction]}$$

$$\hat{\mathbf{x}}(t_k \mid t_k) = \hat{\mathbf{x}}(t_k \mid t_{k-1}) + \mathbf{K}(t_k)\boldsymbol{\varepsilon}(t_k \mid t_{k-1}) \quad \text{[State Correction]}$$

$$\tilde{\mathbf{P}}(t_k \mid t_k) = \left(\mathbf{I} - \mathbf{K}(t_k)\mathbf{C}\right)\tilde{\mathbf{P}}(t_k \mid t_{k-1}) \quad \text{[State Error Covariance Correction]}$$

where

$$\hat{\mathbf{x}}(t_k \mid t_{k-1}) := \mathrm{E}\left\{x(t_k) \mid Y_{t_k}\right\} \text{ and } \tilde{\mathbf{P}}(t_k \mid t_{k-1}) := \mathrm{cov}\left(\tilde{\mathbf{x}}(t_k \mid t_{k-1})\right) \text{ for } \tilde{\mathbf{x}}(t_k \mid t_{k-1}) := x(t_k) - \hat{\mathbf{x}}(t_k \mid t_{k-1})$$

Using the synthesized noisy scintillator/photomultiplier data shown in Fig. 5 we applied the model-based processor (MBP) of Table 2.0 with the results shown in Fig. 7. The performance of the processor is optimum when the innovations sequence is deemed statistically white. The results of this run are in fact *white* indicating optimal performance as shown in Fig. 8.

In Fig. 7, we observe the results of the MBP estimates: the current and voltage outputs. Here we see the smoothed estimates with the predicted uncertainties. The current is reasonable but the predicted error bound are clearly under-estimated while the voltages lie well within the predicted uncertainty bounds. In Fig. 8 we see the underlying performance metrics for this realization of the MBP with the innovations sequence lying within the predicted bounds and the optimality test (zero-mean/bounded covariance) well with the prescribed bounds (0.00008<0.12000 & 2.7% out) with the weighted-sum squared residual (WSSR) statistic below the threshold both indicating a "tuned" optimal processor for this data realization.

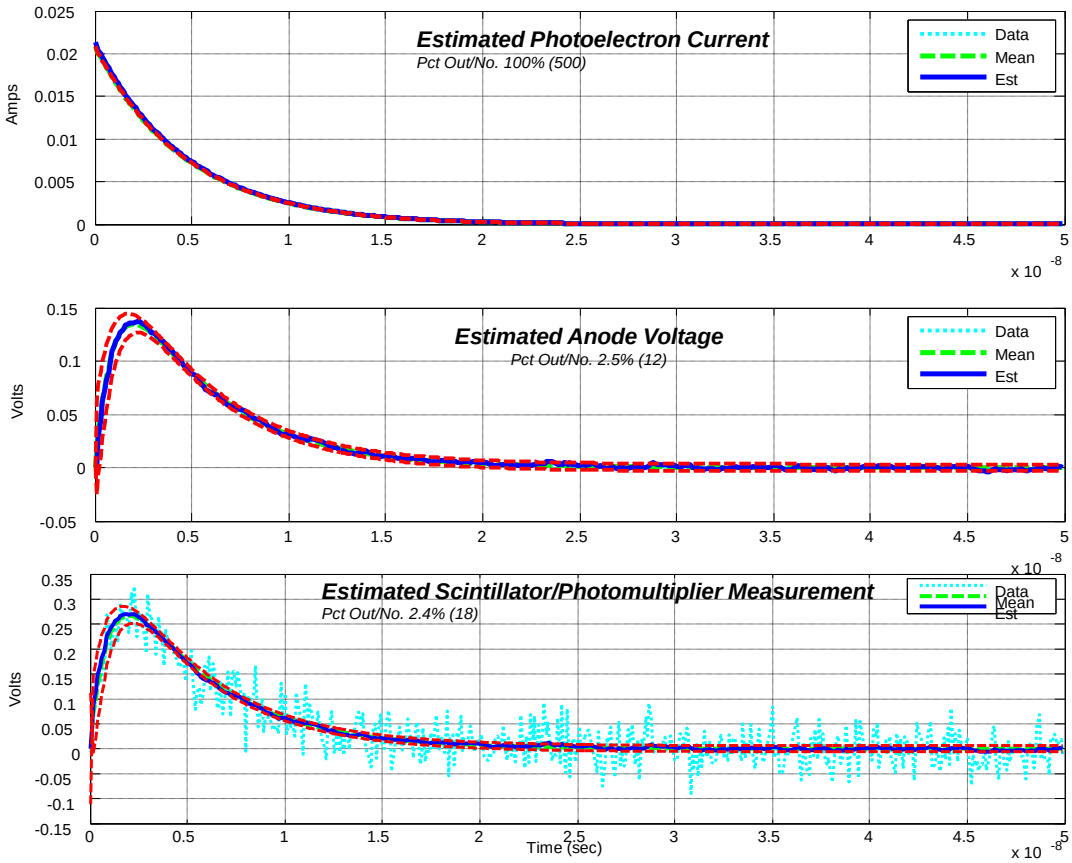

Figure 7. *Estimated outputs for cascaded scintillator/photomultiplier system data: (a) Photoelectron current (100% out). (b) Anode voltage (2.5% out). (c) Measured output voltage (2.4% out).*

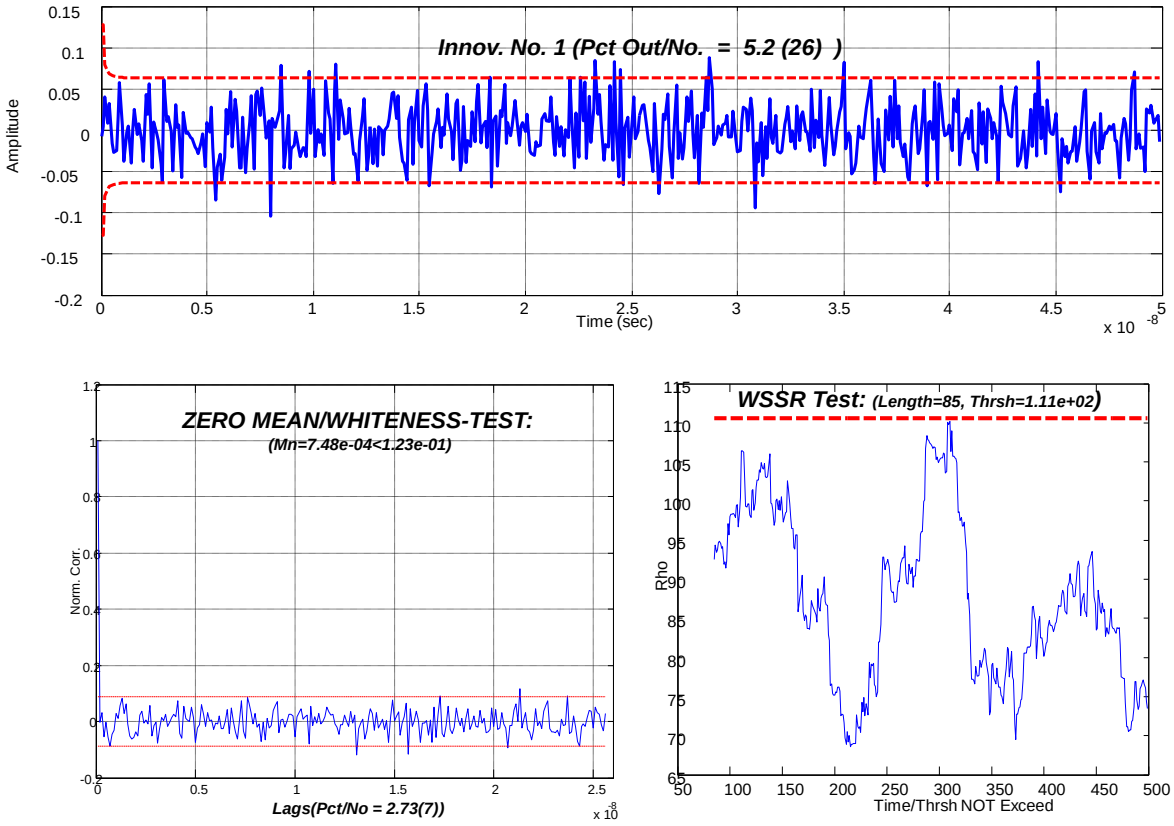

Figure 8. *Performance metrics for MBP: (a) Innovation (5.2% out). (b) Whiteness test (0.0008<0.1200 & 2.7% out). (c) WSSR Test (below threshold).*

MODEL-BASED PROCESSOR: SCINTILLATION /PHOTOMULTIPLIER DATA

In this section we applied the MBP of the previous section to the noisy uncertain measurement data of Fig. 5. Here the parameters of the MBP are adjusted to "track" the raw impulse data and the results are shown in Fig. 9 and 10. In Fig. 9 we observe the estimation of the photoelectron current, anode voltage and output voltage of the PMT unit. The estimates are quite reasonable and the predicted statistics (after re-tuning the MBP) also track the estimated signals. Of course, these results are not considered valid unless the performance metrics (zero-mean/white innovations) are met. The performance is shown in Fig. 10 where we see that the criteria are met satisfactorily with the innovations sequence lying within the predicted bounds, the zero-mean/whiteness test being satisfied (0.0012<0.123/4.9% out) and the WSSR statistic lying beneath its predicted threshold. Thus, we have developed a MBP capable of extracting the noisy scintillation/photomultiplier data and predicting the underlying statistics.

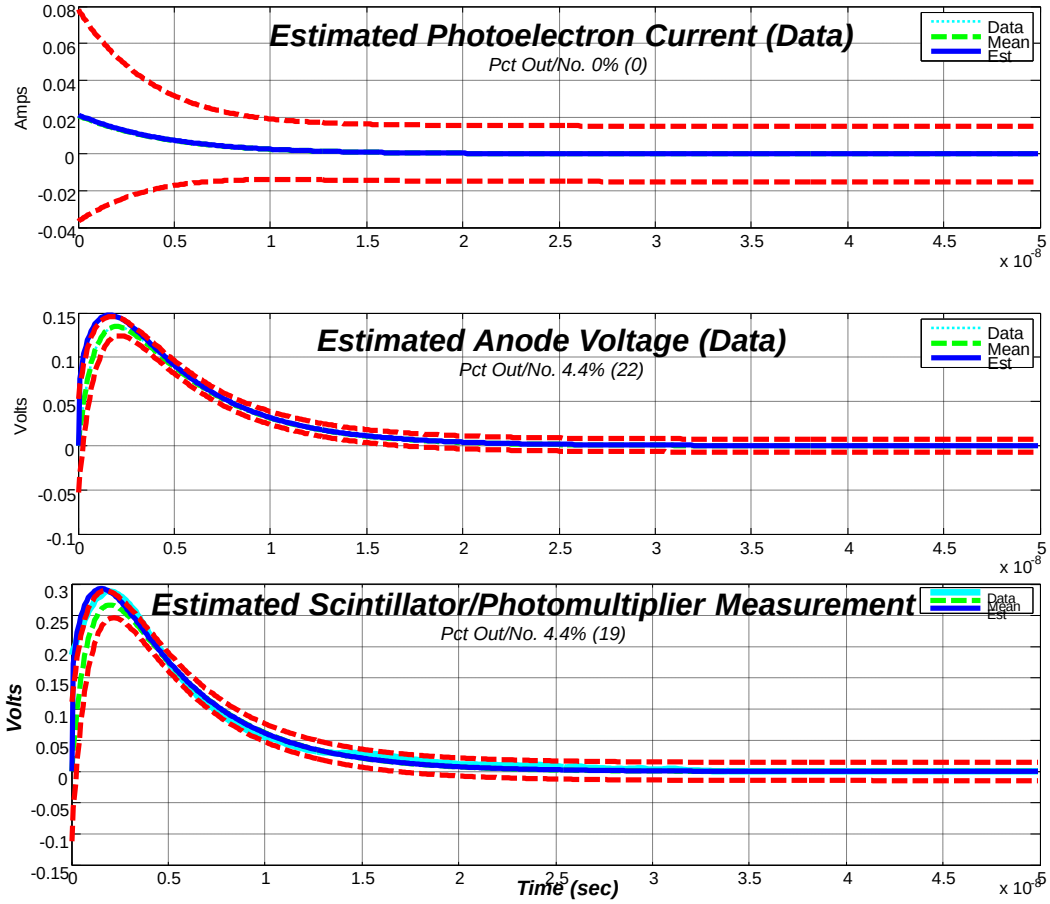

Figure 9. *MBP Estimation for Scintillator Voltage Response: (a) Photoelectron current (0.0% out). (b) Anode voltage (4.4% out). (c) Scintillator/Photomultiplier output voltage (4.4% out).*

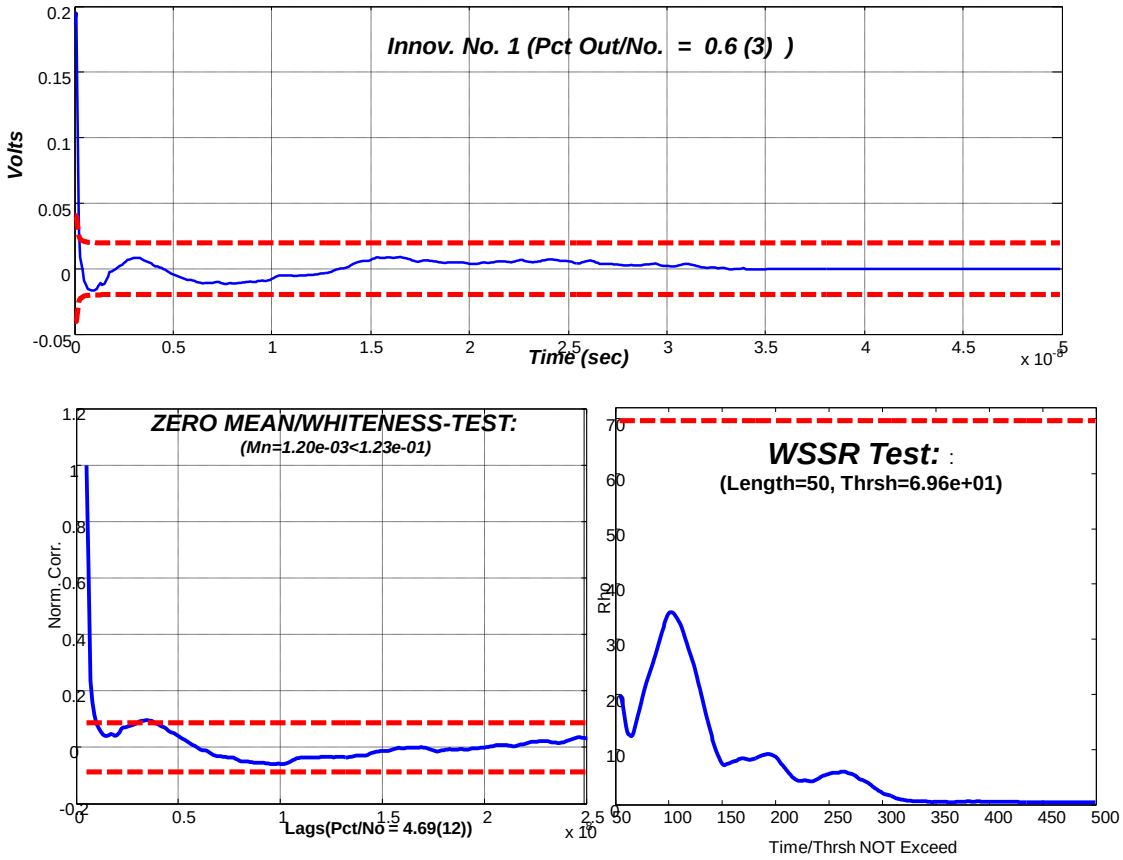

Figure 10. *MBP Performance for Scintillator Voltage Response: (a) Innovations sequence (0.6% out). (b) Zero-mean/whiteness test (0.0012<0.123/4.7% out). (c) WSSR statistic (below threshold).*

REFERENCES

[1] G. Gilmore and J. Hemingway, *Practical Gamma-Ray Spectrometry*, John Wiley & Sons: New York, 2003.

[2] G. F. Knoll, *Radiation Detection and Measurement*, 3rd Ed., John Wiley & Sons: New York, 2000.

[3] R. A. DeCarlo, *Linear Systems: A State Variable Approach with Numerical Implementation*, Prentice-Hall: New Jersey, 1989.

[4] J. V. Candy, *Model-Based Signal Processing*, John Wiley & Sons: New York, 2006.

[5] The MathWorks, *MATLAB Users Manual*, Boston, MA, 1993.

[6] A. V. Oppenheim and R. W. Schafer, *Discrete-Time Signal Processing*, Prentice-Hall: New Jersey, 1989.

[7] W. Kester, D. Sheingold and J. Bryant, *Data Conversion Handbook*, Elsevier, 2005.

ACKNOWLEDGEMENTS

This work performed under the auspices of the U.S. Department of Energy by Lawrence Livermore National Laboratory under Contract DE-AC52-07NA27344.